Carbohydrate Research 380 (2013) 81–91

Contents lists available at ScienceDirect

Carbohydrate Research

journal homepage: www.elsevier.com/locate/carres

Synthesis of new pyrimidine-fused derivatives as potent and selective antidiabetic α-glucosidase inhibitors

Farhad Panahi [a,b], Reza Yousefi [a,*], Mohammad Hossein Mehraban [a], Ali Khalafi-Nezhad [b,*]

[a] Protein Chemistry Laboratory (PCL), Department of Biology, College of Sciences, Shiraz University, Shiraz, Iran
[b] Department of Chemistry, College of Sciences, Shiraz University, Shiraz 71454, Iran

ARTICLE INFO

Article history:
Received 21 June 2013
Received in revised form 20 July 2013
Accepted 21 July 2013
Available online 6 August 2013

Keywords:
α-Glucosidase
Inhibitors
Antidiabetic
Pyrimidine-fused heterocycles

ABSTRACT

The synthesis of a set of pyrimidine-fused derivatives (**L1**–**L8**), resulting from the incorporation of different fragments on the pyrimidine-fused heterocycle (PFH) of the earlier reported α-glucosidase (α-Gls) inhibitor (**C1**–**C5**), allowed the discovery of new ligands with modest and selective inhibitory activity. The PFH core (substructure **2**) was proved to play a significant role in their inhibitory properties. Additionally, the substituent on substructures **1** and **3** of the heterocyclic ring was demonstrated to be important in the enzyme inhibitory action of the pyrimidine-fused derivatives. Moreover, these ligands show selective inhibitory properties for α-Gls over porcine pancreatic α-amylase (α-Amy) which is important in terms of their reduced susceptibility for the possible development of intestinal disturbance side effects. Therefore, low to moderate α-Amy inhibition with effective α-Gls inhibitory action may offer a better therapeutic strategy. Overall, these compounds can potentially offer a new opportunity to develop novel antidiabetic drugs with selective inhibitory action against α-Gls.

1. Introduction

α-Glucosidase (α-Gls) has a crucial role in digestion of carbohydrates and biosynthesis of glycoproteins.[1] Therefore, the inhibition of this enzyme plays an important role in treatment of degenerative diseases such as type-II diabetes mellitus and human immunodeficiency virus (HIV) infection.[2] The inhibitors can reduce the complications of diabetes as they interfere with the enzymatic action of intestinal α-Gls.[3] Consequently, the liberation of glucose into bloodstream will be retarded, resulting in delaying glucose absorption and decreasing postprandial hyperglycemia.[4] In addition, α-Gls inhibition is a promising strategy for development of novel anti-HIV agents, because glycosylation of viral envelope proteins is essential for the virus infectivity.[5] Therefore, during the recent years α-Gls inhibitors have been the imperative entities of various studies in the field of medicinal chemistry.[6–8] Moreover, some α-Gls inhibitors such as Acarbose, Voglibose, and Miglitol have been used as important drugs by diabetic patients.[9] The pseudotetrasaccharide inhibitor Acarbose is a potent pig intestinal sucrase inhibitor with an IC_{50} value of 0.5 mM.[10] However use of Acarbose leads to intestinal disturbances in many patients and there exists a need for development of better and more tolerable α-Gls inhibitors. The selectivity of α-Gls inhibitors is of great importance, as the non-specific inhibition of other Gls especially pancreatic α-Amy may lead to accumulation of non-digested carbohydrates, which in turn results in abdominal cramping, diarrhea, and flatulence.[3]

The pyrimidine ring is an important chemical moiety which can be seen in the molecular scaffold of a large number of alkaloids, drugs, antibiotics, agrochemicals, and antimicrobial agents.[11] Moreover, simple and biologically active pyrimidine fused heterocycles (PFH) such as purine and pteridine are existed in the chemical structure of many natural compounds.[12,13] Also, some of the PFH derivatives are used as antileukemic drugs[14] or potassium-conserving diuretics.[15] A number of fused thieno[3,2-*d*]pyrimidines serves as anti-allergy drugs and others act as fungicides.[11] Additional to inflammatory properties and antioxidant effects, PFH compounds demonstrate further biological activities such as anticancer, antimicrobial, and antiviral actions.[16,17] However, their inhibitory activity against α-Gls was not investigated yet with the exception of our recent study which proved for the first time that PFH based compounds demonstrate inhibitory action against α-Gls.[17] The chemical structure of the synthesized PFH-based α-Gls inhibitors is shown in Figure 1.

Our studies revealed that some of the synthesized compounds not only revealed inhibitory activity toward type-I (yeast) α-Gls, but also they demonstrate potent inhibitory action against type-II (mammalian) enzyme counterpart.[17] Also, PFH-based compounds with aromatic substitution (**C3**) revealed a strong inhibitory activity against both α-Gls. This compound demonstrated an improved inhibitory action on the yeast enzyme

* Corresponding authors. Fax: +98 711 2280916 (R.Y.); fax: +98 711 2280926 (A.K.-N).
E-mail addresses: ryousefi@shirazu.ac.ir (R. Yousefi), khalafi@chem.susc.ac.ir (A. Khalafi-Nezhad).

0008-6215/$ - see front matter © 2013 Elsevier Ltd. All rights reserved.
http://dx.doi.org/10.1016/j.carres.2013.07.008

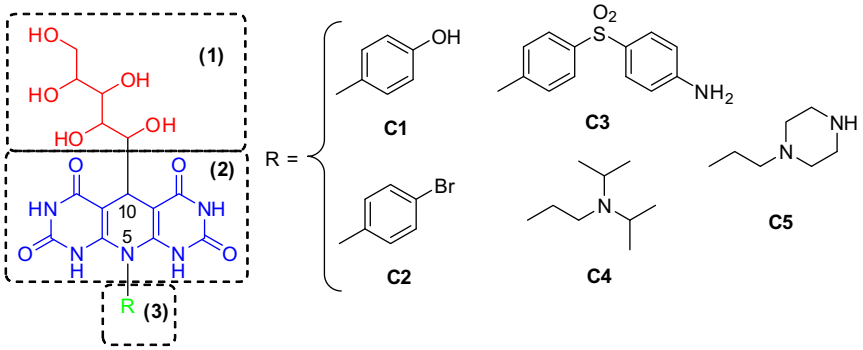

Figure 1. The chemical structure of synthetic PTH-based inhibitors of α-Gls.

compared to the widely applied inhibitor drug of acarbose (28-fold stronger).[17] In addition, the aliphatic substitutions (**C4** & **C5**) exhibited no significant inhibition against yeast and mammalian α-Gls.[17] As shown in Figure 1, this scaffold has three available substructures for further optimization of the inhibitory properties. In design of ligands **C1**–**C5**, our speculation was that the poly hydroxyl chain has an important role in the inhibitory action. In this study we revealed that the PFH (substructure **2**) has a significant role in the inhibitory activity, although the effect of substitution in substructures **1** and **3** was also determinable. Therefore, in the course of searching for the novel, more specific, and easy accessible α-Gls inhibitors, we examined PFH derivatives of different aromatic moieties in the substructures **1** and **3** (Fig. 1). Herein, we report the chemical synthesis and α-Gls inhibitory properties of PFH compounds and discuss the enzymatic mechanism of their inhibition. In order to get a better understanding of their selective inhibition, the effect of these compounds on porcine pancreatic α-amylase (α-Amy) was also examined. Furthermore, circular dichroism (CD) and fluorescence spectroscopy were conducted to obtain a deeper insight into the interaction between the ligands and yeast α-Gls.

2. Results and discussion

2.1. Synthesis of pyrimidine-fused heterocycle derivatives

From the historical point of view, there are three general synthetic methods for the synthesis of pyrimidine-fused derivatives in the literature.[18,19] In the Bischler's strategy the synthesis of PFH is achieved from *ortho*-acetamidobenzaldehyde derivatives.[18] The second method is the Riedel's synthesis, which PFH compounds can be obtained via reductive cyclization of bisformamido derivatives of *ortho*-nitrobenzaldehydes.[19] The so-called Niementowski's synthesis involves preparation of fused pyrimidines from the anthranilic acid derivatives.[18] In modern organic synthesis these compounds have been synthesized using multicomponent reactions (MCRs).[20] MCRs are attractive synthetic strategies, as complex products are formed in a single step and the diversity can be achieved simply by varying the reaction components.[20] Thus, functionally-substituted starting materials can be used to synthesize the desired biologically active compounds.[21] The syntheses of new PFH analogues remain challenging, especially when optimizing their activities. Hence, MCRs represent useful procedures for this goal, because by simply changing the starting material, a large number of pyrimidine-fused analogues with convenient optimization and range of biological activities can be synthesized. The following multicomponent reaction was used to synthesis PFH ligands **L1**–**L7** (Scheme 1). It is noteworthy that the products are precipitated after production and so they are isolated from reaction mixture by simple filtration with high purity.

In this protocol barbituric acid was treated with amines and aldehydes. By changing the amine and aldehyde components a set of PFHs were synthesized. In the selection of aldehyde components, it was decided to use only two aldehydes isovanillin and 3-indole carboxaldehyde, because they have been used as a chemical source in synthesis of many biological active compounds.[22,23] For the synthesis of ligands **L1**–**L3,** 4-bromo-aniline was used as an amine component, because this chemical moiety previously showed α-Gls inhibitory activity in the structure of ligand **C2** (Fig. 1). In the synthesis of ligands **L4**–**L7** a series of bi-functionalized aromatic amines was applied to produce a set of PFH with free NH_2 group in their structures. **L4**–**L7** was synthesized according to our previous ligands as they have been demonstrated significant inhibitory activity against α-Gls. Moreover, it is noteworthy to mention that the free amino groups in their structures can possibly improve their ability for hydrogen bonding interaction. In this class of compounds, one equivalent of amine component was used. However, in one case in order to synthesize a new derivative based on ligand **L5**, 0.5 equiv of amine component was used in the reaction (Scheme 2). This green and efficient reaction was performed in refluxing EtOH in the presence of catalytic amount of tungstophosphoric acid (TPA) as catalyst.[24]

The synthesized compounds **L1**–**L8** were also characterized, using different spectroscopic techniques such as ^{1}H NMR, ^{13}C NMR, infrared (IR), and mass spectroscopy. The data clearly revealed that these molecules were produced successfully. As the purity of synthetic compounds examined using elemental analysis, they were highly pure (>97%).

2.2. The inhibitory activity of pyrimidine fused compounds against α-Gls

The inhibitory activity of eight synthetic ligands (pyrimidine-fused derivatives) against yeast and mouse α-Gls was assessed based on the method described in the experimental section. Also mode of inhibition was determined by Lineweaver–Burk and Cortes plots. To discover the pharmaceutical characteristics of the promising inhibitors, their corresponding IC_{50} values were calculated by Dixon plots. Also Acarbose which is a widely used antidiabetic drug with inhibitory action against mammalian α-Gls was used to serve as the positive control.

In our previous study, we proved that the introduction of poly hydroxyl chain in pyrimidine fused heterocycle compound results in generation of a synthetic compound with significant inhibitory action against both yeast and mouse α-Gls. The replacement of poly hydroxyl chain group with 3-hydroxy-4-methoxy-phenyl and 1*H*-indol-3-yl substitutions (in ligand **C2**) resulted in the production of ligands **L1** and **L2**, respectively (Scheme 1). However, these ligands did not exhibit any inhibitory action. Also, the replacement of oxo group in **L2** with thioxo to produce ligand **L3**

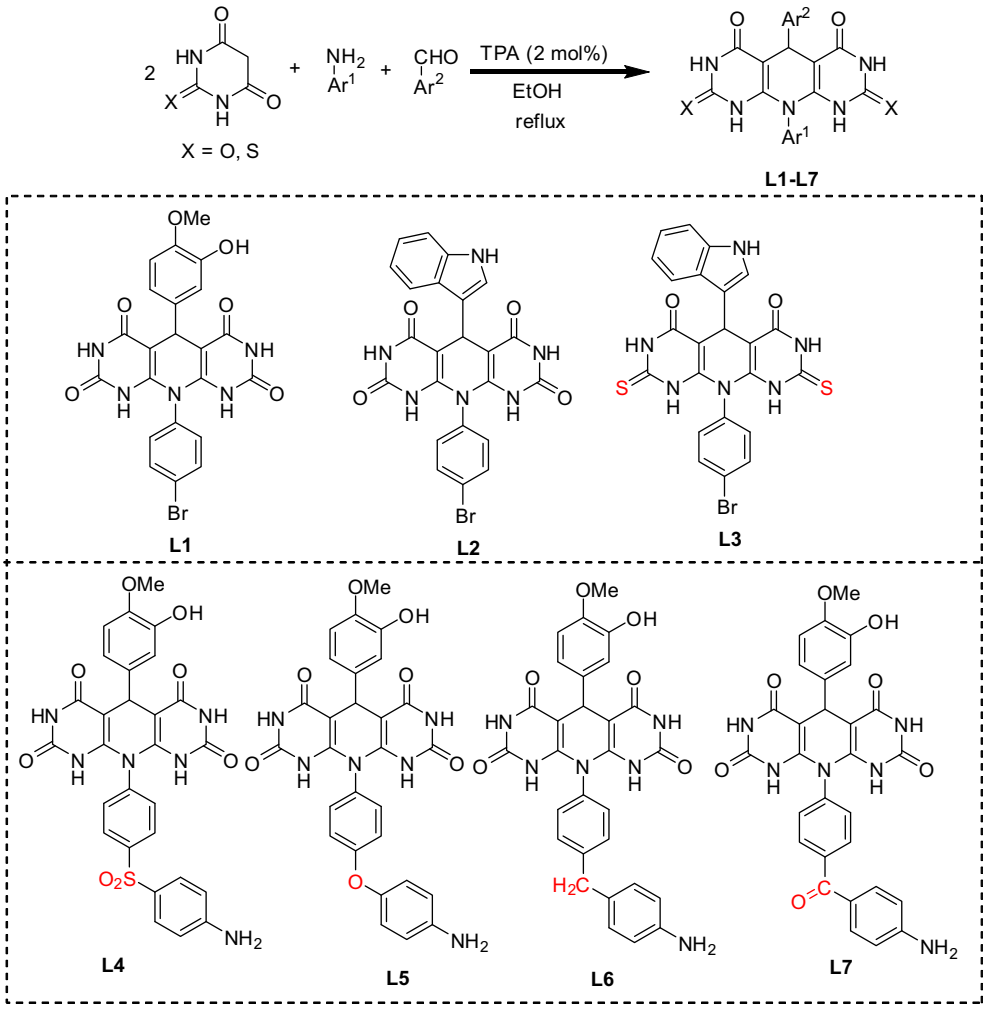

Scheme 1. The synthetic route for the synthesis of ligands **L1**–**L7**.

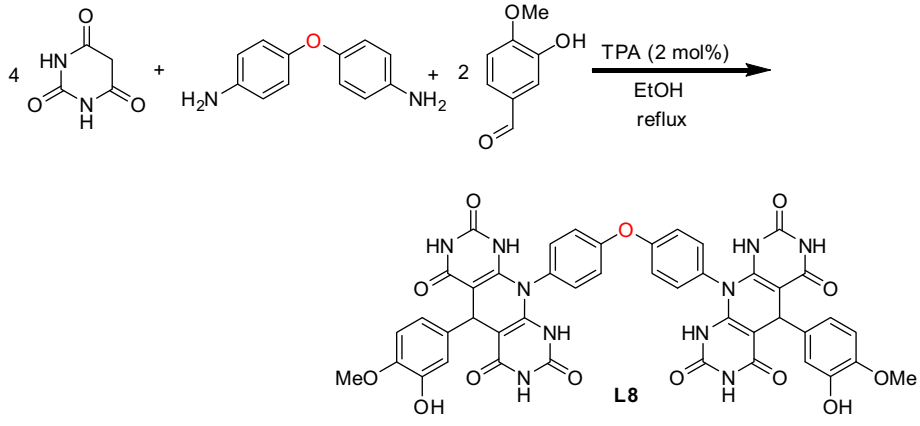

Scheme 2. One-pot synthesis of ligand **L8**.

did not show any effect, suggesting that the latter has no significant effect on the inhibitory action of the synthetic compounds. According to the results of synthetic compounds applied in our previous study (Fig. 1), **C3** with the substituted moiety as '4-(4-aminophenylsulfonyl) phenyl' (4-APSP) revealed strong inhibitory activity with non-competitive and competitive inhibition mode against yeast and mouse α-Gls, respectively. Thus, as shown in Scheme 1, **L4** was synthesized based on **C3** with replacement of the poly hydroxyl chain with 3-hydroxy-4-methoxy-phenyl (the solvability of **L1** was better than **L2**). To our surprise, **L4** did not show any inhibitory activity against these enzymes. So here, the obtained results demonstrate that the activities of compounds are highly depended on poly hydroxyl chain substitution. Therefore, **L5** was synthesized based on chemical structure of **L4**

as following: SO_2 group in **L4** was replaced with the ether linkage in **L5** (Scheme 1) and as a result of this modification, **L5** demonstrated inhibitory activity against both yeast and mouse α-Gls, with the IC_{50} values of 148 ± 1 and 159 ± 3 μM, respectively (Table 1). In spite of the poor inhibition results obtained herein, they clearly indicated that in the absence of poly hydroxyl chain moiety, only by changing of the substitution in substructures **1** and **3** (Fig. 1), one can optimize the inhibitory properties of PFH compounds. It is clear that in the structure of **L5**, there are both hydrogen bonds donating and accepting moieties; acting as a hydrogen donor/acceptor which is one of the most important features of α-Gls inhibitors. The ligands **L4** and **L5** are different only in the hinge-like connection (in substructure **3**) of the main structure. Considering this issue, we decided to synthesize **L6** and **L7** by changing the connecting group, using corresponding amine component in the designed reaction (Scheme 1). Interestingly, **L6** with a 4-(4-aminobenzyl) benzenamine moiety demonstrates the highest inhibitory activity against yeast α-Gls with an IC_{50} value of 9 ± 1 μM (Table 1). However, due to the structural difference of the target enzymes, this ligand did not show any inhibitory activity against mouse α-Gls.

More importantly, **L7** similar to **L4** demonstrated a weak inhibitory activity with an IC_{50} value of 376 ± 1 μM against yeast α-Gls. Also, comparable to **L6**, this ligand (**L7**) did not inhibit mouse α-Gls (Table 1). Comparing the inhibition results of **L4**–**L7**, it can be suggested that rigidity of the group connecting two phenyl moieties in these synthetic ligands is an important factor for their inhibitory action (Scheme 1 and Table 1). The molecular flexibility index of an inhibitor is important for the optimal protein–ligand interaction and enzyme inhibition.[25] Therefore, the critical degree of molecular flexibility which would contribute to the effective enzyme inhibition can be obtained precisely from the modified ligands with proper connecting group.[26] It seems that in ligands **L5** and **L6** the level of rigidity is less than ligands **L4** and **L7**, because the created rigidity by $–SO_2–$[27] and –CO–[28] groups is higher than $–CH_2–$[29] and –O–[30] linkers, so these ligands can easily interact with the corresponding binding residues of protein in the proper connection (Fig. 2).

The optimized molecular structures for the most stable conformation of the synthesized compounds are shown in Figure 3.

As shown, the flexibility of ligands **L5** and **L6** allows them to obtain different morphologies to the other structures which may affect the interaction of these ligands to their corresponding binding sites on the protein.

The selective inhibitory properties of **L6** and **L7** against yeast α-Gls can be raised from the particular structural constraint of their target enzyme.

Overall, the results show that for the inhibitory activity of synthetic ligands the PFH ring is essential, but by selecting the appropriate fragments in substructures **1** and **3**, we can synthesize potent and selective α-Gls inhibitors. For instance, accumulation of another PFH moiety to **L5** as shown in Scheme 2, increases significantly the inhibitory properties of the obtained compound (**L8**) against both yeast and mouse enzymes. According to their corresponding IC_{50} values as reported in Table 1, **L8** demonstrates the inhibitory action 1.9- and 4-fold stronger than **L5** on inhibition of mouse and yeast α-Gls, respectively. This result also demonstrates the effect of PFH structure on the inhibitory properties of the synthetic ligands.

The double reciprocal lineweaver–burk plots of inhibition of the synthetic compounds on yeast and mouse α-Gls are shown in Figures 4 and 5, respectively. As shown in Figure 4, **L5** and **L6**–**L8** inhibit, respectively, the yeast enzyme with mixed-uncompetitive and mixed-competitive modes.

Figure 5 shows the inhibition mechanism of **L5** and **L8** against mouse α-Gls in which both of the ligands demonstrate a mixed-competitive type of inhibition. The inhibitory parameters of the synthetic compounds are illustrated in Table 1.

2.3. Pancreatic α-Amy inhibition

The effects of synthetic compounds against porcine pancreatic α-Amy activity were examined with a concentration higher than their IC_{50} values for yeast and mouse α-Gls. As depicted in Figure 6, a maximum reduction of 20% in activity of α-Amy was observed in the presence of **L6**. Other synthetic ligands demonstrate even lower inhibitory action against this enzyme. Hence, in comparison with Acarbose (70% inhibition), these ligands weakly inhibit the activity of pancreatic α-Amy.

The specific inhibitors of human pancreatic α-Amy have potential as oral agents for the control of blood glucose levels in the treatment of diabetes and obesity.[31] Nonetheless, it is important to mention here that α-Amy breaks down starch into disaccharides that are acted upon by isomaltases, especially α-Gls to release glucose. The presence of potent α-Gls inhibitory activity therefore appears more important in controlling the release of glucose from disaccharides in the gut than α-Amy inhibition. However, moderate α-Amy inhibition with potent α-Gls inhibitory activity may offer better therapeutic strategy that could slowdown the availability of dietary carbohydrate substrate for glucose production in gut, reducing the level of possible intestinal disturbance side effects. Therefore, from these views, the synthetic compounds seem to offer plausible structure–activity relationship.

2.4. Fluorescence investigation of the interaction between yeast α-Gls and the synthetic inhibitors

Fluorescence studies were conducted to obtain a better understanding of the interaction between these compounds and yeast α-Gls. The K_{sv}, K_a, n, and thermodynamic values ΔG, ΔH, and ΔS are summarized in Table 2. Quenching mechanisms are classified in two groups as the following: in dynamic quenching the Stern–Volmer constant is expected to increase with the elevation of temperature; in contrast, as temperature increases the Stern–Volmer constant decreases in the static quenching.[32] The latter was proved to be the quenching mechanism during the interaction of **L6**, **L7**,

Table 1
The IC_{50}, K_i and inhibition mode of the synthetic compounds.

Entry	IC_{50} (μM)		K_{ic} (μM)		K_{im} (μM)		Mode of inhibition	
	Yeast	Mouse	Yeast	Mouse	Yeast	Mouse	Yeast	Mouse
L5	148 ± 1	159 ± 3	222 ± 1.5	86 ± 2.5	37 ± 1.5	370 ± 3	Mixed Un.[a]	Mixed Co.[b]
L6	9 ± 1	–	8 ± 1	–	7 ± 1	–	Mixed Co.	–
L7	376 ± 1	–	333 ± 2	–	500 ± 2	–	Mixed Co.	–
L8	37 ± 1	84 ± 2	31 ± 1	48 ± 2.5	43 ± 1.5	167 ± 3	Mixed Co.	Mixed Co.
Acarbose	296 ± 1	11 ± 1	–	–	–	–	Competitive	–

[a] Competitive binding modes
[b] Uncompetitive binding modes

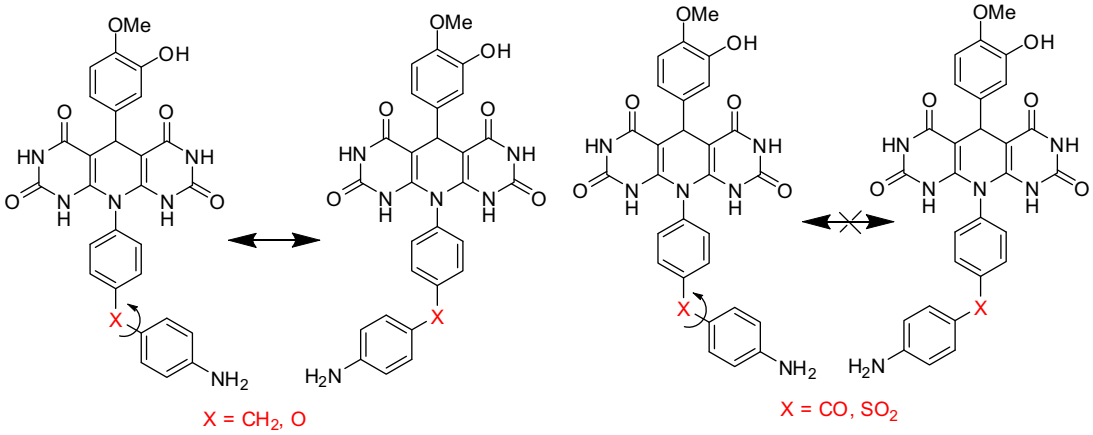

Figure 2. A perspective of molecular rigidity and flexibility in synthetic ligands **L4**–**L7**.

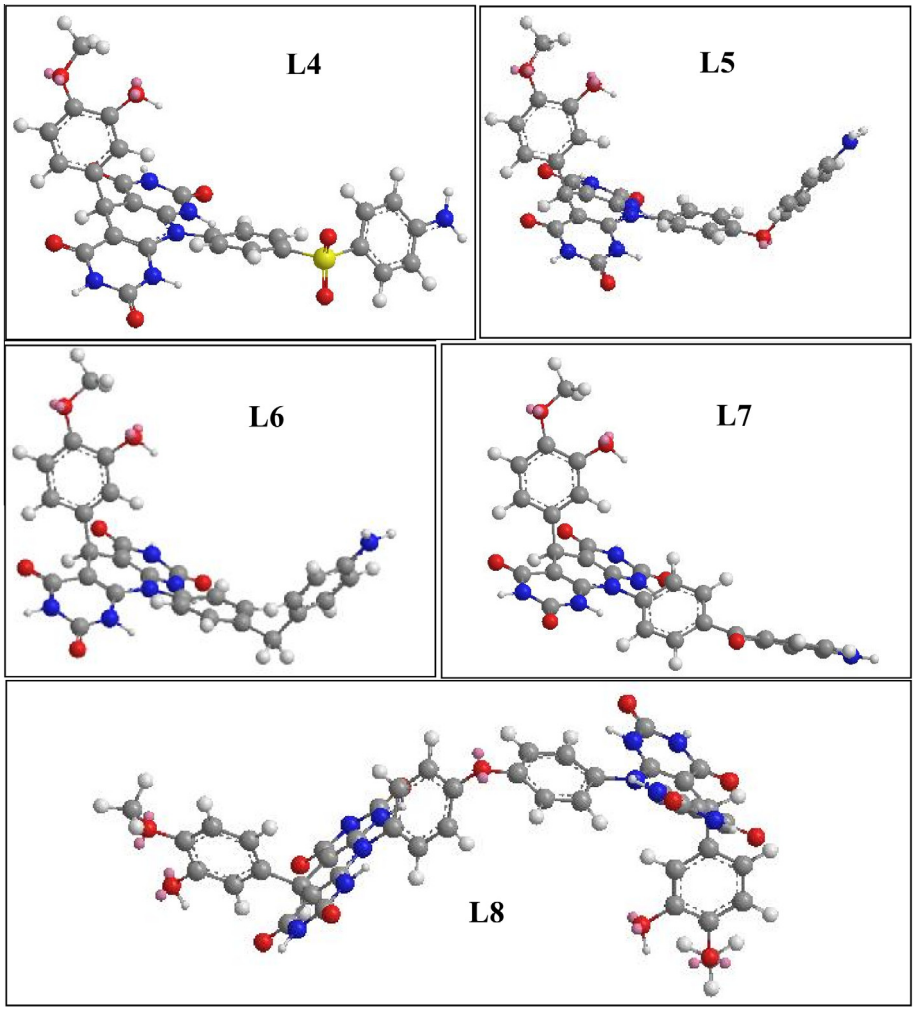

Figure 3. Optimized molecular structures of ligands **L4**–**L8** by AM1 method (using Chembio 3D Ultra 11.0 software).

and **L8** with yeast α-Gls (Figs. 7 and 8). However, the interaction of **L5** with yeast α-Gls was through dynamic quenching mode. Also, the inhibitor–enzyme complex formed by **L6**, **L7**, and **L8** was accompanied by the negative enthalpy changes (Table 2). According to the rules summarized by Ross and Subramanian,[33] the negative ΔH values are observed whenever there is hydrogen bonding in the interaction between ligand and protein. These results prove that the hydrogen bonding may be the driven force of the enzyme–inhibitor complex formation which is in good agreement with our speculation on their hydrogen donor/acceptor abilities as mentioned above. Therefore hydrogen bonding may stimulate the interaction of these inhibitors and yeast α-Gls, resulting in the improved inhibition of the enzyme. Furthermore, the negative values of ΔS in the interaction of **L7** and **L8** prove that vander waals forces

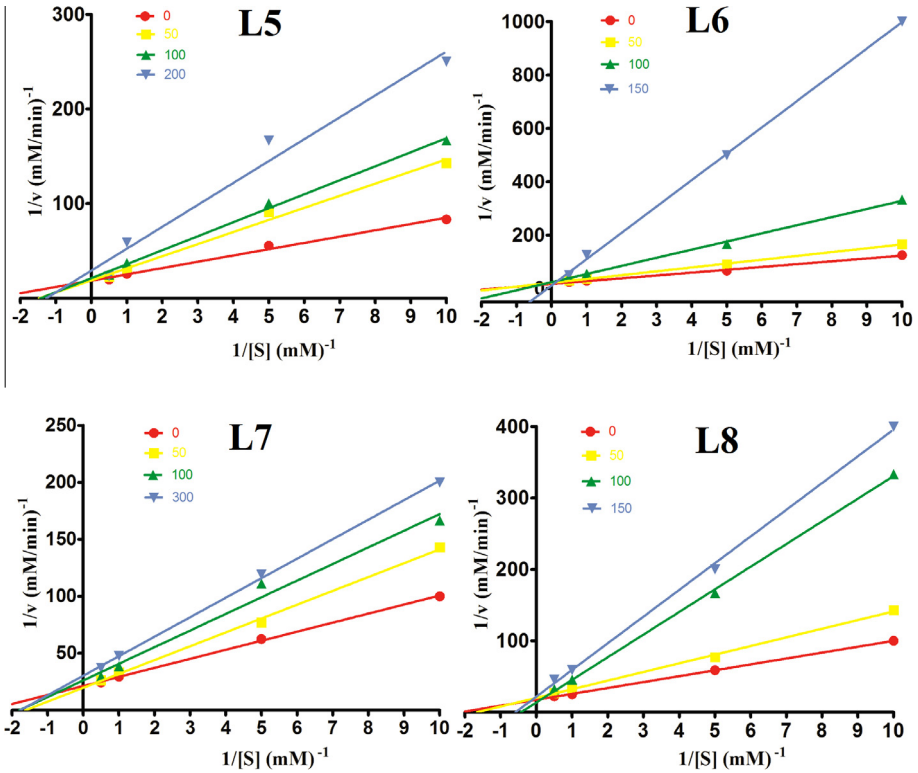

Figure 4. The lineweaver–Burk plots derived from the inhibition of yeast α-Gls by the synthetic compounds **L5**, **L6**, **L7**, and **L8**. The α-Gls activity was measured as a function of pNPG concentration (0.1–2 mM) in the absence and presence of inhibitors (0–300 μM). The experiments performed in 100 mM NaPi buffer, pH 7.0 at 25 °C for 10 min. The different symbols represent the absence (●) and presence (♦, ▼, ■) of these inhibitors in the reaction mixtures.

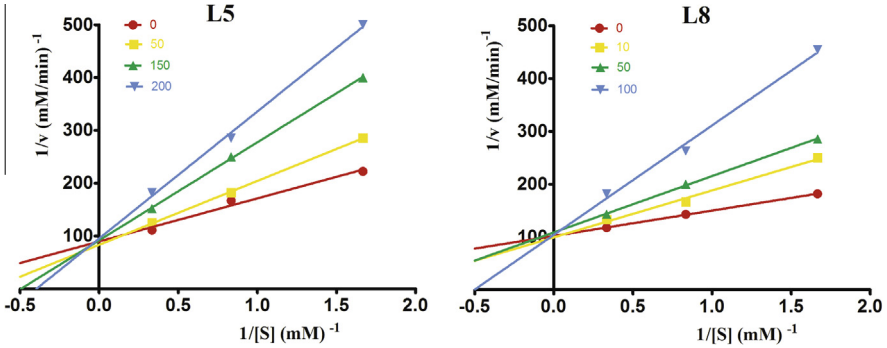

Figure 5. The lineweave–Burk plots derived from the inhibition of mouse α-Gls by synthetic compounds **L5** and **L8**. The α-Gls activity was measured as a function of pNPG concentration (0.6–3 mM) in the absence and presence of inhibitors (0–200 μM). The experiments performed in 10 mM NaPi buffer, pH 7.0 at 37 °C for 30 min. The different symbols represent the absence (●) and presence (♦, ▼, ■) of inhibitor in the reaction mixtures.

may have a minor role in the ligand–inhibitor interaction (Table 2). Values of ΔH and ΔS of the interaction of **L5** and yeast α-Gls were both positive, suggesting contribution of a typical hydrophobic interaction during binding of this inhibitor to the yeast enzyme (Table 2). The negative values of ΔG demonstrated the easy formation of inhibitor–enzyme complex and spontaneity of the interaction. Based on the calculated binding constants, the order of binding at 25 °C (the same as enzyme inhibition assays) was **L8** > **L5** > **L6** > **L7**.

2.5. Secondary structure assessment of yeast α-Gls in the presence of synthetic inhibitors

We recorded the far-UV CD spectra of yeast α-Gls in the absence and presence of different concentrations (20–80 μM) of the ligands (Fig. 9). Yeast α-Gls has a content of 11.8% α-helical structures, 46.9% β-sheets, and 41.3% random coils.[34] Upon interaction, no meaningful structural alteration was induced by the synthetic compounds in this enzyme. Therefore, it is likely that the structural perturbation of yeast α-Gls is not involved in the inhibition mechanism of the synthetic pyrimidine-fused derivatives.

3. Conclusion

In conclusion, a set of pyrimidine-fused heterocycles (eight compounds) with a diversity of molecular structures were synthesized based on the previously reported α-Gls inhibitors.[17] For synthesis of these compounds, a convenient and efficient method via a three-component condensation reaction of aldehydes, amines, and barbituric acid was described. This reaction

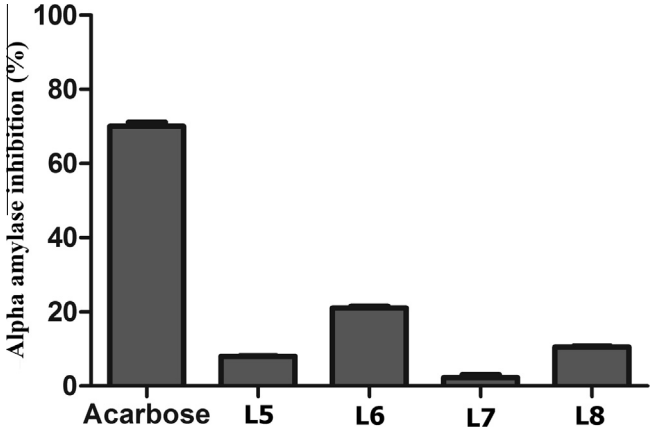

Figure 6. The inhibitory activity of the synthetic compounds against porcine pancreatic α-Amy.

proceeded smoothly in good to excellent yields and the pure products were separated from the reaction mixture by simple filtration. Since the inhibition of α-Gls has become a perfect target in treatment of diabetes especially type-II and AIDS/HIV control, the activities of all compounds were investigated, demonstrating that both PFH ring and the substituents on substructures **1** and **3** of the heterocyclic ring (Fig. 1) play a significant role in the inhibitory activity of these ligands. The results of structure–activity relationships suggest that the rigidity/flexibility of hinge-like connection in substructure **3** of ligands **L4**–**L7** plays an important role in their α-Gls inhibitory action. Also, compound **L8** with a two PFH moiety shows a significant ability for inhibition of mouse α-Gls, suggesting that PFH core plays a significant role in the inhibitory properties of the synthetic ligands. Compared to Acarbose, these ligands weakly inhibit the activity of pancreatic α-Amy. Overall, these compounds can be considered as a foundation for synthesizing novel α-Gls inhibitors which may

Table 2
The thermodynamic parameters, calculated binding and Stem–Volmer constant and the number of bound molecules of the ligands per α-glucosidase molecule (n).

Entry	T	K_{sv} (L mol^{-1})	K_A (L mol^{-1})	n	ΔH (KJ mol^{-1})	ΔG (KJ mol^{-1})	ΔS (J mol^{-1}K^{-1})
L5	298	0.16×10^6	4×10^4	1.28	71.83	−26.62	0.331
	304	0.35×10^6	12×10^4	1.33		−29.57	
	310	0.38×10^6	14×10^4	1.2		−30.57	
L6	298	0.43×10^6	1.8×10^4	1.8	−95.67	−24.27	5.83
	304	0.2×10^6	7×10^4	1.18		−28.19	
	310	0.06×10^6	8×10^4	0.9		−29.1	
L7	298	2.99×10^6	0.2×10^4	1.72	−153.26	−30.31	−0.411
	304	0.78×10^6	0.08×10^4	1.55		−28.59	
	310	0.09×10^6	0.01×10^4	1.38		−25.35	
L8	298	0.9×10^6	7×10^4	1.63	−57.84	−27.69	−0.1
	304	0.35×10^6	5.4×10^4	1.50		−27.56	
	310	0.18×10^6	2.8×10^4	1.44		−26.47	

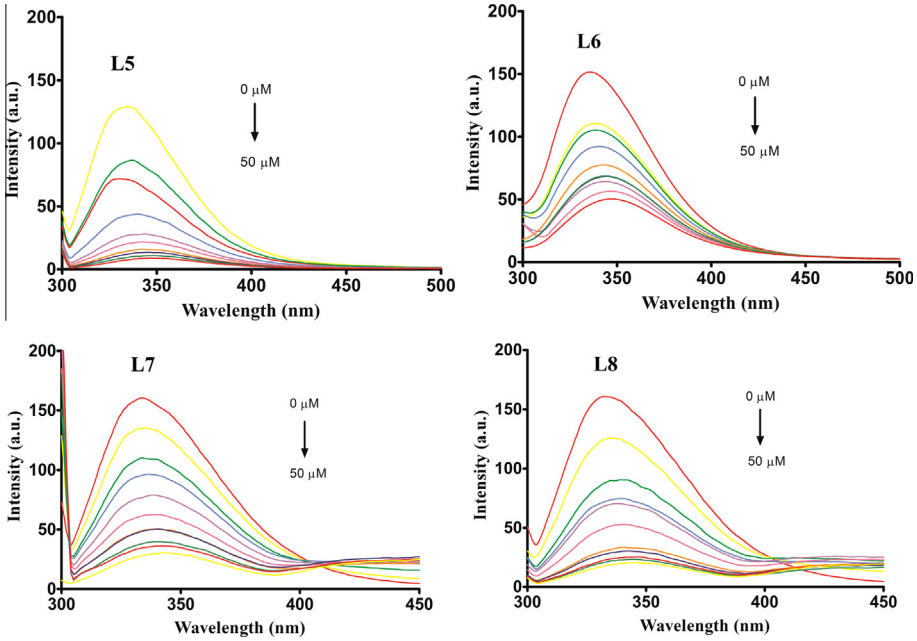

Figure 7. The fluorescence emission spectra of ligand/α-Gls complexes **L5**, **L6**, **L7**, and **L8** at 31 °C. A constant concentration of 0.1 mg/mL yeast α-Gls and different concentrations of ligands (0–50 μM) were used. The reaction performed in 100 mM NaPi buffer pH 7.0 at 25, 31, and 37 °C.

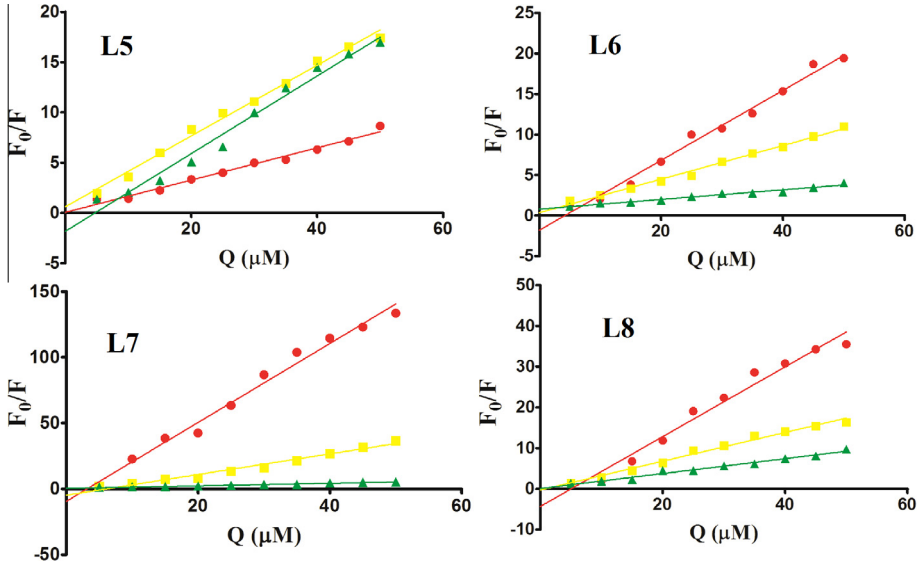

Figure 8. Stern–Volmer plot for the binding of ligands **L5**, **L6**, **L7**, and **L8** with yeast α-Gls. Data for 298 K (●), 304 K (■) and 310 K (▲) are shown.

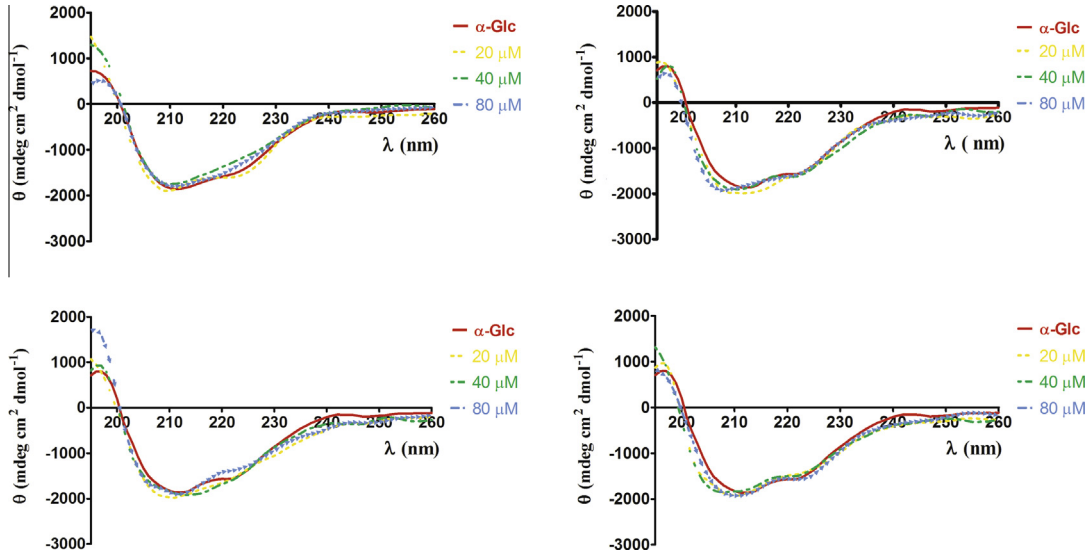

Figure 9. Far-UV CD spectra of yeast α-Gls in the presence of the inhibitors **L5**, **L6**, **L7**, and **L8**. Protein concentration was 0.2 mg/mL and inhibitor concentrations of 20, 40, and 80 μM were added in 100 mM NaPi buffer pH 7.0.

efficiently and specifically inhibit α-Gls and more importantly they may cause less side effects compared to the conventional α-Gls inhibitors such as Acarbose. Further studies on the structure–activity relationship of PFHs are in progress in our laboratories to improve bioactivity of these compounds for achieving more promising α-Gls inhibitors.

4. Experimental section

4.1. Chemistry

4.1.1. General

Chemicals were purchased from Fluka and Aldrich chemical companies and used without further purification. ^{1}H and ^{13}C NMR spectra were recorded on a Bruker Avance 250 MHz spectrometer in DMSO solution with TMS as an internal standard. GC/MS: Shimadzu GC/MS-QP 1000-EX apparatus; in *m*/*z* (rel%) was used for mass analysis of products. FTIR spectroscopy (Shimadzu FT-IR 8300 spectrophotometer) was employed for the ligand characterization. Melting points were determined in open capillary tubes in a Barnstead Electrothermal 9100 BZ circulating oil melting point apparatus. The reaction monitoring was accomplished by TLC on silica gel PolyGram SILG/UV254 plates.

4.1.2. General procedure for preparation of ligands L1–L7

A mixture of barbituric acid (0.26 g, 2 mmol), aldehyde (1 mmol), amine (1 mmol), and $H_3PW_{12}O_{40}$ (0.04 g, 2 mol %) in ethanol (5 mL) at 80 °C was stirred for 12 h. As completion of the reaction confirmed by TLC (eluent EtOAc/MeOH), the reaction mixture was cooled to room temperature. Then, the precipitated product was filtered and washed with water (2 × 10 mL) and ethanol (2 × 5 mL) to afford the pure product.

4.1.3. 9-(4-Bromo-phenyl)-10-(3-hydroxy-4-methoxy-phenyl)-9,10-dihydro-1*H*,8*H*-1,3,6,8,9-pentaaza-anthracene-2,4,5,7-tetraone (L1)

Yield: 91%; yellow solid; mp >350 °C. IR (KBr): 3315, 3098, 1698, 1680 cm^{-1}. ^1H NMR (250 MHz, DMSO-d_6/TMS): δ = 3.86 (s, 3H, OCH_3), 4.92 (s, 1H, CH), 6.55–6.75 (m, 3H, Ar), 6.80 (d, J = 7.7 Hz, 1H, Ar), 6.93 (d, J = 6.7 Hz, 1H, Ar), 7.21 (d, J = 7.5 Hz, 2H, Ar), 11.13 (s, 2H, NH), 11.25 (s, 2H, NH). ^{13}C NMR (62.9 MHz, DMSO-d_6/TMS): δ = 27.3, 57.6, 80.9, 114.1, 116.6, 118.2, 118.5, 123.9, 132.5, 133.8, 143.8, 146.8, 147.0, 152.1, 162.9, 177.5. MS: 526.03 (46.1%, M^+). Anal. Calcd for $C_{22}H_{16}BrN_5O_6$ (526.30): C, 50.21; H, 3.06; N, 13.31. Found: C, 50.48; H, 3.15; N, 13.44.

4.1.4. 9-(4-Bromo-phenyl)-10-(1*H*-indol-3-yl)-9,10-dihydro-1*H*,8*H*-1,3,6,8,9-pentaaza-anthracene-2,4,5,7-tetraone (L2)

Yield: 90%; yellow solid; mp >350 °C. IR (KBr): 3341, 3112, 1713, 1692 cm^{-1}. ^1H NMR (250 MHz, DMSO-d_6/TMS): δ = 4.95 (s, 1H, CH), 6.25 (d, J = 10.7 Hz, 2H, Ar), 6.72 (d, J = 6.7 Hz, 2H, Ar), 6.92–711 (m, 5H, Ar), 9.46 (br s, 1H, NH), 10.09 (br s, 1H, NH), 11.13 (s, 1H, NH), 11.26 (s, 1H, NH). ^{13}C NMR (62.9 MHz, DMSO-d_6/TMS): δ = 26.3, 80.5, 112.3, 113.5, 114.6, 118.4, 120.5, 121.3, 124.1, 124.8, 132.5, 133.4, 137.3, 146.5, 152.1, 165.6. MS: 519.09 (38.5%, M^+). Anal. Calcd for $C_{23}H_{15}BrN_6O_4$ (519.31): C, 53.20; H, 2.91; N, 16.18. Found: C, 53.53; H, 2.98; N, 16.32.

4.1.5. 9-(4-Bromo-phenyl)-10-(1*H*-indol-3-yl)-2,7-dithioxo-2,3,7,8,9,10-hexahydro-1*H*,6*H*-1,3,6,8,9-pentaaza-anthracene-4,5-dione (L3)

Yield: 89%; yellow solid; mp >350 °C. IR (KBr): 3316, 3117, 1673, 1703 cm^{-1}. ^1H NMR (250 MHz, DMSO-d_6/TMS): δ = 4.89 (s, 1H, CH), 6.60–6.63 (m, 2H, Ar), 7.17–7.34 (m, 3H, Ar), 7.56–7.61 (m, 2H, Ar), 7.86–7.90 (m, 2H, Ar), 8.70 (s, 1H, NH), 9.57 (s, 1H, NH), 12.18 (s, 1H, NH), 12.22 (s, 1H, NH), 12.92 (s, 1H, NH). ^{13}C NMR (62.9 MHz, DMSO-d_6/TMS): δ = 29.0, 96.3, 108.7, 111.0, 113.7, 119.2, 122.7, 125.3, 128.8, 137.7, 143.3, 161.0, 170.2, 183.9. MS: 550.95 (26.8%, M^+). Anal. Calcd for $C_{23}H_{15}BrN_6O_2S_2$ (551.44): C, 50.10; H, 2.74; N, 15.24. Found: C, 50.31; H, 2.82; N, 15.34.

4.1.6. 9-[4-(4-Amino-phenoxy)-phenyl]-10-(3-hydroxy-4-methoxy-phenyl)-9,10-dihydro-1*H*,8*H*-1,3,6,8,9-pentaaza-anthracene-2,4,5,7-tetraone (L4)

Yield: 85%; yellow-orange solid; mp >350 °C. IR (KBr): 3310, 3101, 1708, 1697 cm^{-1}. ^1H NMR (250 MHz, DMSO-d_6/TMS): δ = 3.87 (s, 3H, OCH_3), 4.82 (s, 1H, CH), 6.61-6.71 (m, 5H, Ar), 6.92 (d, J = 6.5 Hz, 1H, Ar), 7.04 (d, J = 7.0 Hz, 2H, Ar), 7.16 (d, J = 8.7 Hz, 1H, Ar), 7.22 (d, J = 6.5 Hz, 1H, Ar), 9.22 (br s, 2H, NH_2), 11.43 (s, 1H, NH), 11.60 (s, 1H, NH), 12.25 (s, 1H, NH), 12.34 (s, 1H, NH). ^{13}C NMR (62.9 MHz, DMSO-d_6/TMS): δ = 27.3, 55.4, 78.9, 115.2, 116.0, 118.2, 119.8, 123.6, 132.3, 140.1, 143.4, 146.9, 147.3, 151.2, 151.5, 166.5. MS: 554.11 (21.2%, M^+). Anal. Calcd for $C_{28}H_{22}N_6O_7$ (554.51): C, 60.65; H, 4.00; N, 15.16. Found: C, 60.78; H, 4.07; N, 15.23.

4.1.7. 9-[4-(4-Amino-benzenesulfonyl)-phenyl]-10-(3-hydroxy-4-methoxy-phenyl)-9,10-dihydro-1*H*,8*H*-1,3,6,8,9-pentaaza-anthracene-2,4,5,7-tetraone (L5)

Yield: 83%; yellow solid; mp >350 °C. IR (KBr): 3374, 3115, 1693, 1677, 935, 807 cm^{-1}. ^1H NMR (250 MHz, DMSO-d_6/TMS): δ = 3.86 (s, 3H, OCH_3), 4.82 (s, 1H, CH), 6.68 (s, 1H, Ar), 6.85 (d, J = 9.5 Hz, 2H, Ar), 7.02 (d, J = 9.2 Hz, 4H, Ar), 7.83 (d, J = 9.5 Hz, 4H, Ar), 9.43 (br s, 1H, OH), 11.12 (s, 2H, NH), 11.25 (s, 2H, NH). ^{13}C NMR (62.9 MHz, DMSO-d_6/TMS): δ = 27.1, 57.0, 80.4, 115.8, 116.8, 118.1, 123.5, 127.9, 129.2, 132.1, 143.5, 146.9, 151.8, 152.5, 166.3. MS: 602.11 (8.9%, M^+). Anal. Calcd for $C_{28}H_{22}N_6O_8S$ (602.57): C, 55.81; H, 3.68; N, 13.95. Found: C, 55.93; H, 3.73; N, 14.06.

4.1.8. 9-[4-(4-Amino-benzyl)-phenyl]-10-(3-hydroxy-4-methoxy-phenyl)-9,10-dihydro-1*H*,8*H*-1,3,6,8,9-pentaaza-anthracene-2,4,5,7-tetraone (L6)

Yield: 85%; yellow solid; mp >350 °C. IR (KBr): 3401, 3118, 1691, 1674 cm^{-1}. ^1H NMR (250 MHz, DMSO-d_6/TMS): δ = 3.72 (s, 3H, OCH_3), 3.86 (s, 2H, CH_2), 4.83 (s, 1H, CH), 6.48 (s, 1H, Ar), 6.64 (d, J = 8.2 Hz, 2H, Ar), 6.80 (d, J = 8.5 Hz, 4H, Ar), 7.00–7.06 (m, 4H, Ar), 10.02 (br s, 1H, OH), 11.11 (s, 1H, NH), 11.14 (s, 1H, NH), 11.26 (s, 2H, NH). ^{13}C NMR (62.9 MHz, DMSO-d_6/TMS): δ = 27.5, 55.7, 78.8, 111.2, 114.4, 118.5, 120.3, 125.3, 129.4, 135.2, 145.6, 150.2, 150.6, 167.7. MS: 552.16 (15.9%, M^+). Anal. Calcd for $C_{29}H_{24}N_6O_6$ (552.54): C, 63.04; H, 4.38; N, 15.21. Found: C, 63.13; H, 4.43; N, 15.39.

4.1.9. 9-[4-(4-Amino-benzoyl)-phenyl]-10-(3-hydroxy-4-methoxy-phenyl)-9,10-dihydro-1*H*,8*H*-1,3,6,8,9-pentaaza-anthracene-2,4,5,7-tetraone (L7)

Yield: 81%; yellow solid; mp >350 °C. IR (KBr): 3396, 3112, 1692, 1675, 14, 1270 cm^{-1}. ^1H NMR (250 MHz, DMSO-d_6/TMS): δ = 3.79 (s, 3H, OCH_3), 4.84 (s, 1H, CH), 6.65 (s, 1H, Ar), 6.85 (d, J = 9.5 Hz, 2H, Ar), 7.02 (d, J = 9.2 Hz, 4H, Ar), 7.83 (d, J = 9.5 Hz, 4H, Ar), 9.43 (br s, 1H, OH), 11.12 (s, 2H, NH), 11.25 (s, 2H, NH). ^{13}C NMR (62.9 MHz, DMSO-d_6/TMS): δ = 27.1, 57.0, 80.4, 115.8, 116.8, 118.1, 123.5, 127.9, 129.2, 132.1, 143.5, 146.9, 151.8, 152.5, 166.3. MS: 566.08 (27.4%, M^+). Anal. Calcd for $C_{29}H_{22}N_6O_7$ (566.52): C, 61.48; H, 3.91; N, 14.83. Found: C, 61.58; H, 3.99; N, 14.96.

4.1.10. 10-(3-Hydroxy-4-methoxy-phenyl)-9-(4-{4-[10-(3-hydroxy-4-methoxy-phenyl)-2,4,5,7-tetraoxo-1,3,4,5,6,7,8,10-octahydro-*2H*-1,3,8,9-tetraaza-anthracen-9-yl]-10-(3-Hydroxy-4-methoxy-phenyl)-9-phenyl-9,10-dihydro-1*H*,8*H*-1,3,6,8,9-pentaaza-anthracene-2,4,5,7-tetraone (L8)

For synthesis of this compound, a mixture of barbituric acid (0.26 g, 2 mmol), isovanillin (1 mmol), amine (0.5 mmol), and $H_3PW_{12}O_{40}$ (0.04 g, 2 mol %) in ethanol (5 mL) at 80 °C was stirred for 24 h. As completion of the reaction confirmed by TLC (eluent EtOAc/MeOH), the reaction mixture was cooled to room temperature. Then, the precipitated product was filtered and washed with water (2 × 10 mL) and ethanol (2 × 5 mL) to afford the pure product. Yield: 86%; yellow solid; mp >350 °C. IR (KBr): 3385, 3115, 1691, 1701 cm^{-1}. ^1H NMR (250 MHz, DMSO-d_6/TMS): δ = 3.86 (s, 6H, OCH_3), 4.91 (s, 2H, CH), 6.81–6.87 (m, 6H, Ar), 6.94–6.99 (m, 4H, Ar), 7.02–7.13 (m, 4H, Ar), 10.07 (br s, 6H, NH & OH), 11.14 (s, 2H, NH), 11.27 (s, 2H, NH). ^{13}C NMR (62.9 MHz, DMSO-d_6/TMS): δ = 27.7, 57.1, 80.9, 115.5, 116.2, 118.1, 119.0, 123.6, 132.3, 140.5, 143.4, 147.1, 151.9, 152.5, 166.1. MS: 908.08 (4.8%, M^+). Anal. Calcd for $C_{44}H_{32}N_{10}O_{13}$ (908.78): C, 58.15; H, 3.55; N, 15.41. Found: C, 58.38; H, 3.63; N, 15.65.

4.2. Biological experiments

4.2.1. α-Gls inhibitory activity

Yeast α-Gls was available in pure form and used as a model enzyme for investigating the potential inhibitors. The yeast α-Gls assay was conducted based on the previous spectrophotometric method with slight changes.[35] In this assay, 4-nitrophenyl-β-D-glucopyranosiduronic acid (pNPG) was used as substrate and the liberation of *p*-nitrophenol (pNP; the colored reagent) from pNPG was monitored at 410 nm as an indicator of the enzyme activity. The experiments were performed with a T90$^+$ UV/vis spectrophotometer instrument (PG instrument, UK) equipped with Peltier Temperature Controller (Model PTC-2). In brief, 1 U/mL of the yeast enzyme was added to different concentrations of pNPG (0.1–2 mM); then at a constant substrate concentration, the increasing amounts of each inhibitor were added in order to determine the

inhibition mode by Lineweaver–Burk plots. The IC_{50} value of each inhibitor which shows the concentration required for 50% inhibition of α-Gls was calculated using dixon plots,[36] in which the intercepts on the abscissa show the IC_{50} values. The inhibition constants (K_i) were calculated using Cortes method in which the slope of a plot of $1/IC_{50}$ versus V_0/V (relative velocity) shows the inhibition constant.[36] The results of inhibition of both yeast and mammalian α-Gls are summarized in Table 1. The mouse enzyme is a type II α-Gls which is located in the brush border of intestinal cells. To assay the activity of this enzyme, we used the intestinal acetone powder and the assay was conducted according to our previous publication.[17] Briefly, 10 μL of the enzyme solution was added to a sample solution containing the synthetic compounds and pNPG, and the release of *p*-nitrophenol (pNP) from pNPG monitored at 410 nm for 30 min at 37 °C. The inhibition mode was determined by incubating mouse α-Gls (0.3 units/mL) in the presence of increasing concentrations of pNPG (0.6–3 mM) and different concentrations of each synthetic inhibitor.

4.2.2. Pancreatic α-Amy inhibition assay

The α-Amy inhibition was determined based on conventional methods.[3] In this study, type VI-B porcine pancreatic α-Amy was used. Based on this assay, 1 mg/mL of the maltose solution (pH 6.9) can be hydrolyzed by 1 unit of this enzyme for 3 min at 20 °C. A total of 500 μL of each inhibitor and 500 μL of 20 mM NaPi buffer (pH 6.9 with 6 mM NaCl), containing α-Amy solution (0.5 mg/mL) were incubated at 25 °C for 10 min. The synthetic ligands were used with a concentration higher than their IC_{50} values for yeast and mouse α-Gls (200 μM). After pre incubation, 500 μL of a 0.5% starch solution in 20 mM NaPi buffer (pH 6.9 with 6 mM NaCl) was added to each tube at timed intervals. The reaction was stopped with 1.0 mL of dinitrosalicylic acid color reagent. The test tubes were then incubated at 90 °C in a water bath for 10 min and cooled down to the room temperature. The reaction mixture was then diluted 1:10 with double distilled water, and absorbance was measured at 540 nm with a $T90^+$ UV/vis spectrophotometer. The readings were compared with the controls, containing buffer instead of sample extract. The results were expressed as percentage of α-Amy inhibition.

4.2.3. Fluorescence spectroscopy

Fluorometric studies were carried out on a Cary-Eclipse spectrofluorimeter (Model Varian, Sydney, Australia). Solution of yeast α-Gls (0.1 mg/mL) was prepared in 100 mM NaPi buffer pH 7.0. Also stock solution of the inhibitors (5 mM) was made in 0.1 M NaOH. Lower concentrations of the inhibitors were made from the above stock by dilution. Samples with constant concentration of yeast α-Gls (0.1 mg/mL) and different concentrations (0–50 μM) of each inhibitor were mixed. The fluorescence spectra were recorded at λ_{exc} = 290 nm and λ_{em} from 300 to 500 nm. Trp emission intensity at 330 nm was used to calculate the binding parameters due to the previous publication.[37] To analyze the interaction of the yeast α-Gls and inhibitors the quenching constant K_{sv} was determined using the Stern–Volmer equation:

$$\frac{F_0}{F} = 1 + K_{sv}[Q] \quad (1)$$

where F_0 and F are relative fluorescence of α-Gls in the absence and presence of the inhibitors, Q is the concentration of the quencher (inhibitor) and K_{sv} is the quenching constant. The binding constant (K_A) and the number of binding sites (n) on the yeast α-Gls were calculated using the following equation:

$$\log\frac{F_0 - F}{F} = \log K_A + n\log[Q] \quad (2)$$

The inner filtration effect was eliminated using the equation below:

$$F_{Cor} = F_{obs}10^{A_1+A_2} \quad (3)$$

where F_{cor} and F_{obs} are the correct and observed intensities however, A_1 and A_2 are the sum of α-Gls and the inhibitor absorbance at the excitation and emission wavelengths, respectively.[38]

Thermodynamic parameters are the main clue to confirm the binding force of the interaction namely hydrogen bonds, van der Waals force, hydrophobic bonds, electrostatic interactions, etc. If the enthalpy change (ΔH^θ) does not vary significantly over the studied temperature range, its value and that of entropy (ΔS^θ) can be determined by van't Hoff equation:

$$\ln K_A = \frac{\Delta H^\theta}{RT} + \frac{\Delta S^\theta}{R} \quad (4)$$

The free energy change (ΔG^θ) was calculated based on the following equation:

$$\Delta G^\theta = -RT\ln K_A \quad (5)$$

where, R is the gas constant 8.314 J mol^{-1} K^{-1} and T is the temperature (K).

4.2.4. The circular dichroism (CD) experiment

The CD spectra of yeast α-Gls in the presence and absence of the inhibitors were recorded with a CD spectrophotometer instrument (Aviv, Model-215, USA). Far-UV CD region (200–260 nm) was selected to investigate the secondary structure contents of the yeast α-Gls, using 1 mm path cuvettes. The concentration of the enzyme was kept constant (0.2 mg/mL), while varying the inhibitors' concentration (20–80 μM). The results were expressed in molar ellipticity [θ] (deg cm^2/dmol) and molar ellipticity was calculated using the following equation:[39]

$$[\theta] = \frac{MRW \times \theta_{obs}}{10 \times d \times C} \quad (6)$$

where MRW is the mean amino acid residue weight of the α-Gls (116), θ_{obs} is the observed ellipticity in degrees at a given wavelength, d is the length of the cuvette in cm, and C is the concentration of the protein in mg/mL. The secondary structure alteration of the enzyme was predicted using CDNN CD spectra deconvolution software.

Acknowledgments

We would like to thank financial support of Iran National Science Foundation (INSF)-Grant No. 88001894. Also the financial supports of research councils of Shiraz University are gratefully acknowledged.

References

1. Van Beers, E. H.; Büller, H. A.; Grand, R. J.; Einerhand, A. W. C.; Dekker, J. *Crit. Rev. Biochem. Mol. Biol.* **1995**, *30*, 197–262.
2. Shen, Q.; Shao, J.; Peng, Q.; Zhang, W.; Ma, L.; Chan, A. S. C.; Gu, L. *J. Med. Chem.* **2010**, *53*, 8252–8259.
3. Zhang, L.; Hogan, S.; Li, J.; Sun, S.; Canning, C.; Zheng, S. J.; Zhou, K. *Food Chem.* **2011**, *126*, 466–471.
4. Suresh Babu, K.; Tiwari, A. K.; Srinivas, P. V.; Ali, A. Z.; Raju, B. C.; Rao, J. M. *Bioorg. Med. Chem. Lett.* **2004**, *14*, 3841–3845.
5. Ma, C. M.; Hattori, M.; Daneshtalab, M.; Wang, L. *J. Med. Chem.* **2008**, *51*, 6188–6194.
6. Trapero, A.; Llebaria, A. *J. Med. Chem.* **2012**, *55*, 10345–10346.
7. Standl, E.; Schnell, O. *Diabetes Vasc. Dis. Res.* **2012**, *9*, 163–169.
8. Kato, A.; Hayashi, E.; Miyauchi, S.; Adachi, I.; Imahori, T.; Natori, Y.; Yoshimura, Y.; Nash, R. J.; Shimaoka, H.; Nakagome, I.; Koseki, J.; Hirono, S.; Takahata, H. *J. Med. Chem.* **2012**, *55*, 10347–10362.
9. Asano, N. *Glycobiology* **2003**, *13*, 93R–104R.
10. Thomson, R. J.; von Itzstein, M. In *Carbohydrate-based Drug Discovery*; Wong, C.-H., Ed.; Wiley-VCH: Weinheim, 2003; Vol. 2, pp 831–862.
11. Brown, D. J. The Chemistry of Heterocyclic Compounds In *The Pyrimidines*; Wiley-Interscience, 2009; Vol. 52,.

12. Lister, J. H. In *Chemistry of Heterocyclic Compounds*; Wiley-Interscience, 1967; Vol. 24,
13. Brown, D. The Chemistry of Heterocyclic Compounds, Fused Pyrimidines, Part III In *Pteridines*; Taylor, E. C., Ed.; J. Wiley & Sons: New York–Chichester–Brisbane–Toronto–Singapore, 1988; Vol. 24/3,.
14. Albert, A. *Selective Toxicity: The Physico-Chemical Basis of Therapy*; Chapman and Hall London: UK, 1985.
15. Weinstock, J.; Wilson, J. W.; Wiebelhaus, V. D.; Maass, A. R.; Brennan, F. T.; Sosnowski, G. *J. Med. Chem.* **1968**, *11*, 573–579.
16. Mohamed, M. S.; Awad, S. M.; Hiremath, A. I. S. *Molecules* **2010**, *15*, 1882–1890.
17. Yousefi, R.; Alavian-Mehr, M. M.; Mokhtari, F.; Panahi, F.; Mehraban, M. H.; Khalafi-Nezhad, A. *J. Enzyme Inhib. Med. Chem.* **2012**. http://dx.doi.org/10(3109/14756366), 2012, 727812.
18. Armarego, W. *The Chemistry of Heterocyclic Compounds, Fused Pyrimidines*; Wiley-Interscience, 2009.
19. Lister, J. H. The Chemistry of Heterocyclic Compounds, Fused Pyrimidines. In *The Purines*; Wiley-Interscience, 2009.
20. Khalafi-Nezhad, A.; Divar, M.; Panahi, F. *Tetrahedron Lett.* **2013**, *54*, 220–222.
21. Monfardini, I.; Huang, J. W.; Beck, B.; Cellitti, J. F.; Pellecchia, M.; Domling, A. *J. Med. Chem.* **2011**, 890–900.
22. Panoutsopoulos, G. I.; Beedham, C. *Cell. Physiol. Biochem.* **2005**, *15*, 089–098.
23. Gurkok, G.; Altanlar, N.; Suzen, S. *Chemotherapy* **2009**, *55*, 15–19.
24. Khalafi-Nezhad, A.; Panahi, F. *Synthesis* **2011**, 984–992.
25. Hritz, J.; Ruiter, A. D.; Oostenbrink, C. *J. Med. Chem.* **2008**, *51*, 7469–7477.
26. Erickson, J. A.; Jalaie, M.; Robertson, D. H.; Lewis, R. A.; Vieth, M. *J. Med. Chem.* **2004**, *47*, 45–55.
27. Johnson, R. N. Encyclopedia of Polymer Science and Technology In In Herman, F. M., Norman, G. G., Bikales, M. N., Eds.; John Wiley & Sons, Inc.: New York, London, Sydney and Toronto, 1969; Vol. 11, p 447.
28. Wang, W.; Cui, J.; Lu, X.; Padakanti, P. K.; Xu, J.; Parsons, S. M.; Luedtke, R. R.; Rath, N. P.; Tu, Z. *J. Med. Chem.* **2011**, *54*, 5362–5372.
29. Whitlock, B. J.; Whitlock, H. W., Jr. *J. Am. Chem. Soc.* **1985**, *107*, 1325–1329.
30. Bacosca, I.; Hamciuc, E.; Bruma, M. *Soft Mater.* **2013**, *11*, 465–475.
31. Tarling, C. A.; Woods, K.; Zhang, R.; Brastianos, H. C.; Brayer, G. D.; Andersen, R. J.; Withers, S. G. *Chem. Bio. Chem.* **2008**, *9*, 433–438.
32. Ray, A.; Koley Seth, B.; Pal, U.; Basu, S. *Spectrochim. Acta Part A Mol. Biomol. Spectrosc.* **2012**, *92*, 164–174.
33. Ross, P. D.; Subramanian, S. *Biochemistry* **1981**, *20*, 3096–3102.
34. Choi, C. W.; Choi, Y. H.; Cha, M.-R.; Yoo, D. S.; Kim, Y. S.; Yon, G. H.; Hong, K. S.; Kim, Y. H.; Ryu, S. Y. *J. Agric. Food Chem.* **2010**, *58*, 9988–9993.
35. Saijyo, J.; Suzuki, Y.; Okuno, Y.; Yamaki, H.; Suzuki, T.; Miyazawa, M. *J. Oleo Sci.* **2008**, *57*, 431–435.
36. Cortés, A.; Cascante, M.; Cárdenas, M. L.; Cornish-Bowden, A. *Biochem. J.* **2001**, *357*, 263.
37. Schilstra, M. J.; Veldink, G. A.; Vliegenthart, J. F. G. *Biochemistry* **1994**, *33*, 3974–3979.
38. Chi, Z.; Liu, R. *Biomacromolecules* **2010**, *12*, 203–209.
39. Divsalar, A.; Saboury, A.; Yousefi, R.; Moosavi-Movahedi, A.; Mansoori-Torshizi, H. *Int. J. Biol. Macromol.* **2007**, *40*, 381–386.